Eur. Phys. J. C (2022) 82:300
https://doi.org/10.1140/epjc/s10052-022-10237-9

THE EUROPEAN PHYSICAL JOURNAL C

Regular Article - Theoretical Physics

Momentum relaxation of holographic Weyl semimetal from massive gravity

Junkun Zhao[a]

Center for Gravitational Physics, Department of Space Science, Beihang University, Beijing 100191, China

Received: 10 January 2022 / Accepted: 20 March 2022 / Published online: 6 April 2022

Abstract We consider the effects of momentum relaxation on the topological quantum phase transitions in holographic Weyl semimetals. The translational symmetry breaking in the field theory is realized in the framework of massive gravity. The quantum phase transition is between a Weyl semimetal phase and a topological trivial phase, which is controlled by M/b, i.e. the ratio of mass parameter and time reversal symmetry breaking parameter. We find that the critical value of the phase transition $(M/b)_c$, characterized by the anomalous Hall conductivity, decreases with the increasing of graviton mass, i.e. the momentum relaxation strength. There exists a critical value of graviton mass above which the topological phase transition disappears and therefore the Weyl points are destroyed. All these phenomena are qualitatively similar to that of axion fields induced momentum relaxation, indicating that a universal feature emerges in the momentum relaxed holographic Weyl semimetals, which is also consistent with the predictions from weakly coupled field theory.

Contents

[a] e-mail: junkunzhao@buaa.edu.cn (corresponding author)

1 Introduction

Weyl semimetals is a novel topological gapless state of quantum matter where its valence band and conduction band touch at certain points, namely the Weyl nodes, in momentum space [1,2]. These Weyl nodes come in pairs with opposite chirality and are topologically stable under the perturbations that preserve charge conservation or translational symmetry [3]. Close to the Weyl nodes, the low-energy excitations satisfy the relativistic Weyl equation. Therefore, the quasiparticles behave like Weyl fermions which are anomalous quantum mechanically, leading to lots of exotic transport phenomena in Weyl semimetals. Thus, it has attracted numerous theoretical and experimental interest [1–6]. Theoretically, most studies on Weyl semimetals are based on the topological band theory or the weakly coupled field theory. However, similar to graphene system [7], the effective fine structure constant in Weyl semimetal can be large due to the smallness of the fermi velocity which plays the role of speed of light, implying that the Weyl semimetals can be strongly coupled without quasiparticles [8]. This raises the question of theoretical description of strong-interacting Weyl semimetals.

On the other hand, gauge/gravity duality (or AdS/CFT correspondence) provides a novel approach to study the strongly-interacting quantum many-body system [9–11]. The physics is holographically encoded in a weakly-coupled classical gravity living in one higher dimension. The holographic method has been successfully applied to explore various phases and their transports, yielding lots of significant insights. In the case of topological matter, the strongly-coupled holographic Weyl semimetals have been constructed recently [12,13], where the Weyl semimetal phase is characterized by a nonzero anomalous Hall conductivity and there exists a topological quantum phase transition between the

Weyl semimetal phase and a topological trivial phase.[1] Subsequently, the existence of surface states [18] and the calculation of topological invariants [19] in the holographic system reveal the key features of Weyl semimetals. Many more works along this line can be found in [20–34] and see [35] for a recent review on the topic.

In real condensed matter system, the translational symmetry is broken explicitly due to the presence of background lattice, which is important to relax the electron's momentum and give rise to a finite DC conductivities. Holographically, there are several different realizations of translational symmetry breaking, such as by the presence of a periodic lattice [36,37] or by the mean field theory approaches (e.g. helical lattices [38], massive gravity [39], linear axion model [40], Q-lattices [41]). Notably, the translational symmetry breaking has been missed in most studies of holographic Weyl semimetals.[2] This might be due to that holographic Weyl semimetal mainly focus on zero density physics and naively the momentum relaxation only play important role at finite density. However, in weakly coupled field theory descriptions, even at zero density the Weyl points can be annihilated by scattering with other Weyl points of opposite chirality due to the broken of translational symmetry [3]. Therefore, it is natural to study the role of translational symmetry breaking at strong coupling, i.e. in the holographic Weyl semimetals.

Recently, the phenomenon of momentum relaxation in holographic Weyl semimetals has been explored in [32], where the presence of axion fields break the translational invariance [40,42]. It has been found that the Weyl semimetal phase shrinks and eventually ceases to exist with the increasing of momentum relaxation strength. However, there are two questions to be answered. The first question is the zero temperature ground-state of momentum relaxed holographic Weyl semimetals, which has distinct geometry structure because of the nonzero axion fields. It is important to construct the zero temperature solutions in order to reveal the underlying structure of the topological quantum phase transition. The second question is the universality of the effects of momentum relaxation on the system. In weakly coupled field theory [3], the destroy of Weyl nodes should be independent of the mechanism of translational symmetry breaking. It is worth studying different model of translational symmetry breaking to test the universality of the phenomenon. In the present work, we will address the second question.

We will use the massive gravity (see, eg. [39,43–46]) to test the effects of translational symmetry breaking on holographic Weyl semimetal. The bulk diffeomorphism invariance is broken due to the non-zero graviton mass terms, which corresponds to the translational symmetry breaking in the dual field theory. As the absolute zero temperature is not accessible in experiment, we will focus on the finite temperature physics. Even though, the information of quantum phase transition can be obtained due to the existence of quantum critical region. We will mainly focus on the effects of momentum relaxation on the properties of the topological phase transition in holographic Weyl semimetals.

The outline of this paper is as follows. We begin, in Sect. 2, by introducing the holographic model of Weyl semimetal with non-zero graviton mass terms. In Sect. 3, we study the effects of graviton mass on d.c. transports of vector gauge field fluctuations. Section 4 is aimed to the conclusion and discussion. In the Appendix, we present the details of background equations of motion, asymptotic expansions and thermodynamics.

2 Holographic setup

In this section, we introduce the holographic model of Weyl semimetals [12,13] in the presence of non-zero graviton mass terms [39,46]. The action for the model is given by

$$\begin{aligned}\mathcal{S} = \int d^5x\sqrt{-g}\Big[&\frac{1}{2\kappa^2}\Big(R+\frac{12}{L^2}\Big)-\frac{1}{4}F_{ab}F^{ab}\\ &-\frac{1}{4}\mathcal{F}_{ab}\mathcal{F}^{ab}+\frac{\alpha}{3}\epsilon^{abcde}A_a\big(F_{bc}F_{de}+3\mathcal{F}_{bc}\mathcal{F}_{de}\big)\\ &-(D_a\Phi)^*(D^a\Phi)-V(\Phi)+\frac{m_g^2}{2\kappa^2}\sum_{i=1}^{4}c_i\mathcal{U}_i(g,f)\Big]\\ &+\mathcal{S}_{\rm GH}+\mathcal{S}_{\rm c.t.}\,,\end{aligned} \tag{2.1}$$

where κ^2, L and α are the gravitational constant, AdS radius and Chern–Simons coupling respectively. The axial gauge field A_μ is dual to the axial current in the field theory and its field strength is $F_{ab}=\partial_a A_b-\partial_b A_a$. The vector gauge field V_μ is dual to the vector current in the field theory and its field strength is $\mathcal{F}_{ab}=\partial_a V_b-\partial_b V_a$. The Chern–Simons terms are included to characterize the anomalous of the axial symmetry in the field theory. The complex scalar field Φ is axial charged with the covariant derivative $D_a=\partial_a-iqA_a$. We choose the potential of the scalar field as $V(\Phi)=m^2\Phi^2+\frac{\lambda}{2}\Phi^4$ with the scalar field mass $m^2=-3$. The graviton mass terms are linear combination of $\mathcal{U}_i$, where the coefficient c_i are dimensionless constants and m_g is the graviton mass. Note that $\mathcal{U}_i$ are symmetric polynomials of the eigenvalues of the 5×5 matrix $\mathcal{K}^a_{\ b}\equiv\sqrt{g^{ac}f_{cb}}$

$$\begin{aligned}\mathcal{U}_1&=[\mathcal{K}]\,,\\ \mathcal{U}_2&=[\mathcal{K}]^2-[\mathcal{K}^2]\,,\\ \mathcal{U}_3&=[\mathcal{K}]^3-3[\mathcal{K}][\mathcal{K}^2]+2[\mathcal{K}^3]\,,\\ \mathcal{U}_4&=[\mathcal{K}]^4-6[\mathcal{K}^2][\mathcal{K}]^2+8[\mathcal{K}^3][\mathcal{K}]+3[\mathcal{K}^2]^2-6[\mathcal{K}^4],\end{aligned}$$

[1] See [14–17] for the semi-holographic and the top-down approach for strongly-coupled Weyl semimetals.

[2] See [24] for a study of quenched disorder on holographic Weyl semimetals in the probe limit.

where the rectangular brackets denote traces: $[\mathcal{K}] = \mathcal{K}^a_a$. In massive gravity, the dynamical metric g_{ab} couples to the symmetric reference metric f_{cd}, which breaks diffeomorphism invariance and gives the graviton a mass. In our coordinates (t, x, y, z, r), we choose the reference metric $f_{cd} = \text{diag}(0, F, F, F_z, 0)$ with constant F and F_z. Thus the spatial reparameterization symmetry is broken, which results in the momentum relaxation in the field theory. $\mathcal{S}_{\text{GH}}$ is the standard Gibbons–Hawking term and $\mathcal{S}_{\text{c.t.}}$ is the counterterm to make the physical observable finite. For simplicity, we will concentrate on the case of $q = 1$ and $\lambda = 1/10$ in this paper.

We set $2\kappa^2 = 1$. The bulk equations of motion are

$$
\begin{aligned}
&R_{ab} - \frac{1}{2}g_{ab}\big(R + 12\big) - m_g^2\chi_{ab} - \frac{1}{2}T_{ab} = 0\,,\\
&\nabla_b\mathcal{F}^{ba} + 2\alpha\epsilon^{abcde}F_{bc}\mathcal{F}_{de} = 0\,,\\
&\nabla_b F^{ba} + \alpha\epsilon^{abcde}(F_{bc}F_{de} + \mathcal{F}_{bc}\mathcal{F}_{de})\\
&\quad + iq[\Phi(D^a\Phi)^* - \Phi^*(D^a\Phi)] = 0\,,\\
&D_aD^a\Phi - m^2\Phi - \lambda(\Phi^*)^2\Phi = 0\,.
\end{aligned}
$$

where

$$
\begin{aligned}
\chi_{ab} = {}& \frac{c_1}{2}\big(\mathcal{U}_1 g_{ab} - \mathcal{K}_{ab}\big)\\
&+\frac{c_2}{2}\big(\mathcal{U}_2 g_{ab} - 2\mathcal{U}_1\mathcal{K}_{ab} + 2\mathcal{K}^2_{ab}\big)\\
&+\frac{c_3}{2}\big(\mathcal{U}_3 g_{ab} - 3\mathcal{U}_2\mathcal{K}_{ab} + 6\mathcal{U}_1\mathcal{K}^2_{ab} - 6\mathcal{K}^3_{ab}\big)\\
&+\frac{c_4}{2}\big(\mathcal{U}_4 g_{ab} - 4\mathcal{U}_3\mathcal{K}_{ab}\\
&+12\mathcal{U}_2\mathcal{K}^2_{ab} - 24\mathcal{U}_1\mathcal{K}^3_{ab} + 24\mathcal{K}^4_{ab}\big)\,,\\
T_{ab} = {}& \left[\mathcal{F}_{ac}\mathcal{F}_b{}^c - \frac{1}{4}g_{ab}\mathcal{F}^2\right]\\
&+\left[F_{ac}F_b{}^c - \frac{1}{4}g_{ab}F^2\right]\\
&+\big[D_a\Phi(D_b\Phi)^* + (D_a\Phi)^*D_b\Phi\big]\\
&-g_{ab}\left[(D_c\Phi)^*(D^c\Phi) + V(\Phi)\right],
\end{aligned}
$$

We make the following ansatz for the background fields

$$
\begin{aligned}
ds^2 = {}& -udt^2 + f(dx^2 + dy^2)\\
&+hdz^2 + \frac{dr^2}{u},\\
A = {}& A_z dz,\ \ \Phi = \phi(r),
\end{aligned}
\tag{2.2}
$$

where u, f, h, A_z, ϕ depend on the radial coordinate r. With the above ansatz, we find[3]

$$
\mathcal{K}_{ab} = \text{diag}\Big(0\ ,\ F\sqrt{f}\ ,\ F\sqrt{f}\ ,\ F_z\sqrt{h}\ ,\ 0\Big)\,, \tag{2.3}
$$

$$
\begin{aligned}
&\mathcal{U}_1 = \frac{2F}{\sqrt{f}} + \frac{F_z}{\sqrt{h}}\,,\quad \mathcal{U}_2 = \frac{2F^2}{f} + \frac{4FF_z}{\sqrt{fh}}\,,\\
&\mathcal{U}_3 = \frac{6F^2F_z}{f\sqrt{h}}\,,\quad \mathcal{U}_4 = 0\,.
\end{aligned}
\tag{2.4}
$$

We can obtain the corresponding equations of motion following the above ansatz and see Appendix A for details. As $r \to \infty$, the background geometry is asymptotically to AdS_5 with $u, f, h \sim r^2 + \cdots$. For the scalar field and the axial gauge field, we have

$$
\phi = \frac{M}{r} + \cdots\,,\qquad A_z = b + \cdots\,, \tag{2.5}
$$

where M and b correspond to the mass parameter and the time-reversal symmetry breaking parameter of the field theory respectively.

2.1 Brief review of holographic Weyl semimetal

Before discussing the effects of momentum relaxation induced by the massive gravity, it is useful to summarise the important ingredients in translation invariant holographic Weyl semimetals [12,13]. In this subsection, we will review the zero and the finite temperature physics of the holographic Weyl semimetals and focus on their properties of phase transition.

At zero temperature, we have $u = f$ which corresponds to Lorentz invariance in the field theory along the (t, x, y) direction. We have only one tunable dimensionless parameter M/b. By tuning M/b, we can find three phases with different infrared solutions [12]: (I) *the Weyl sememetal phase* exists when $M/b < (M/b)_c$, (II) *the Lifshitz critical point* exists when $M/b = (M/b)_c = 0.744$, (III) *the topological trivial phase* exists when $M/b > (M/b)_c$. These three phases are distinguished by anomalous Hall conductivity, which is nonzero in the Weyl semimetal phase while vanishes in the topological trivial phase and the critical point. With the increasing of M/b, the system experiences a topological quantum phase transition from the Weyl semimetal phase to a topological trivial phase and see Fig. 1 for the phase diagram. Note that, the anomalous Hall conductivity is proportional to the near horizon value of the axial gauge field, i.e. $\sigma_{AHE} \propto A_z(0)$, which is the order parameter of the quantum phase transition.

At finite temperature, the infrared (IR) fixed points are covered by black hole horizon, where the background fields admit a regular expansion near the horizon. The topological quantum phase transition now becomes a smooth crossover due to thermal correlations. In particular, the anomalous Hall conductivity has a very small value in the topological trivial phase and the quantum critical point produces a quantum

[3] In holographic Weyl semimetals, for a non-trivial profile of A_z, the systems are anisotropic with $f \neq h$. Therefore, the $\mathcal{U}_1$ and $\mathcal{U}_2$ typically contain two terms, which is different from the isotropic cases [46]. Thus, even for $c_1 = c_3 = 0$ and $c_2 \neq 0$, the model we studied here is distinct from [32], which can also be seen more directly by comparing the background equations of motion of these two models.

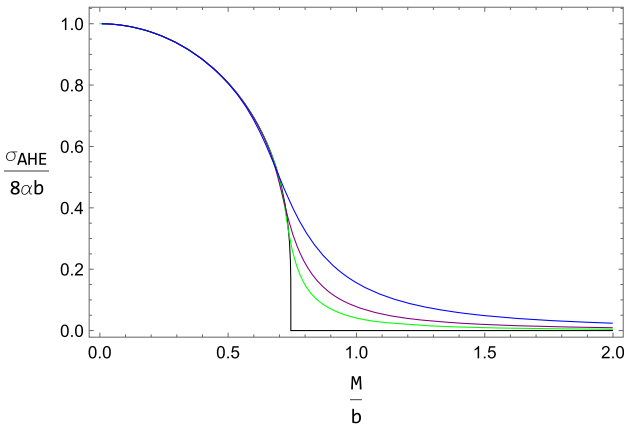

Fig. 1 The anomalous Hall conductivity as a function of the M/b in the minimal holographic Weyl semimetals [12]. The black line corresponds to the zero temperature while the colored lines correspond to the finite temperature with $T/b = 0.05$ (blue), 0.03 (purple), 0.02 (green) respectively. At finite temperature, the sharp quantum phase transition becomes a crossover

critical range at finite temperature. Even though, we can still obtain the critical point of phase transition from the behavior of anomalous Hall conductivity. We define the point M/b with maximal $|\frac{\partial\sigma_{AHE}}{\partial(M/b)}|$ as the critical value of the phase transition, which will approach to the critical point of topological quantum phase transition as the temperature is decreased. For example, the critical value at $T/b = 0.02$ is 0.722 with a relative error within 3% compared with the zero temperature result. Therefore, we will use this method to identify the critical point of the phase transition in the following study.

2.2 Holographic Weyl semimetal with massive gravity

In this subsection, we will obtain the equilibrium solutions with non-zero graviton mass terms by solving the background equations of motion. It is reasonable to postulate that there still exists a quantum phase transition from the Weyl semimetal phase to a topological trivial phase. We will focus on the finite temperature physics of the momentum relaxed holographic Weyl semimetals.

Before studying the finite temperature physics, let us point out one important fact. From the tt and rr component of Einstein equation, we know[4]

$$\left[\sqrt{h}(u'f - uf')\right]' = -m_g^2\left[6F^2F_zc_3 + 2FF_zc_2\sqrt{f} + 2F^2c_2\sqrt{h} + Fc_1\sqrt{fh}\right]. \tag{2.6}$$

In the translation invariant case, i.e. $m_g = 0$, the right hand side is zero. The above equation saturates the null energy condition (NEC), which requires $\left[\sqrt{h}(u'f - uf')\right]' \geq 0$. From this equation, we can also define a radially conserved Noether charge $Q = \sqrt{h}(u'f - uf')$, which gives $Q = Ts$ at the black hole horizon. Consequently, the zero temperature solution (i.e. for $u = f$) is equivalent to $Q = 0$. However, in the presence of non-zero graviton mass terms, we can not convert (2.6) into a total derivative and the $u = f$ condition for ground-state is not applicable. The situation here is similar to the case in Ref. [32], indicating that the zero temperature ground-state has different geometries with $u \neq f$. Therefore, the study of ground state demands more works and we will leave it for further study.

Additionally, we can restrict the value of c_i, $(i = 1, 2, 3)$ from (2.6). The observation is that the right hand side of (2.6) should be positive in order to maintain the NEC in the $m_g \to 0$ limit. In the case where only one of c_i is nonzero, this restriction requires $c_i < 0$.[5]

Now, we begin our study of the finite temperature physics, where the system is specified by five dimensionless parameters M/b, T/b and $m_g|c_i|/b$, $(i = 1, 2, 3)$. Without loss of generality, we will focus on the $\mathcal{U}_2$ sector of massive gravity by tuning the parameter c_2 and fixing $m_g = 1$.[6] We further fix the temperature $T/b = 0.03$ and the reference metric $F = F_z = 1$. Therefore, the system now has two dimensionless parameters M/b and $m_g|c_2|/b$. The infrared (IR) and ultraviolet (UV) expansions for the background fields can be found in the Appendix A. For given initial seeds, the background solutions can be obtained by integrating the equations of motion from IR towards UV.

Specifically, in the Weyl semimetal phase, we find that the background fields flow differently from UV to IR for different graviton mass. This is illustrated in Fig. 2, where we show the profile of ϕ and A_z for different graviton mass at $M/b = 0.01$. In the translation invariant case (i.e. $m_g = 0$, the black dashed lines), the axial gauge field keeps a constant value, while the scalar field first increases, then decreases to zero from the boundary towards the horizon, showing a non-monotonic behavior. In the non-zero graviton mass case, however, the axial gauge field turns out to decrease monotonically from the boundary to the horizon. The scalar field shows a transition from a non-monotonic function to a monotonic increasing function from the boundary towards the horizon. Especially, as the graviton mass is increased, the near horizon value of A_z decreases while the near horizon value of ϕ increases. Therefore, the presence of non-zero graviton mass terms can lead to a dramatic change of the flow of matter fields. This signals that an emergent phenomenon occurs in the Weyl semimetal phase under momentum relaxation,

[4] This is the first equation of the full background equations of motion in the Appendix A.

[5] It is possible to have positive c_i in the parameter space by considering more nonzero c_i.

[6] As we have discussed below (2.3), due to the anisotropic of holographic Weyl semimetal, the system we studied in this paper is distinct from [32], even for $c_2 \neq 0$, $c_1 = c_3 = 0$. For this reason, it is proper to consider $c_2 \neq 0$.

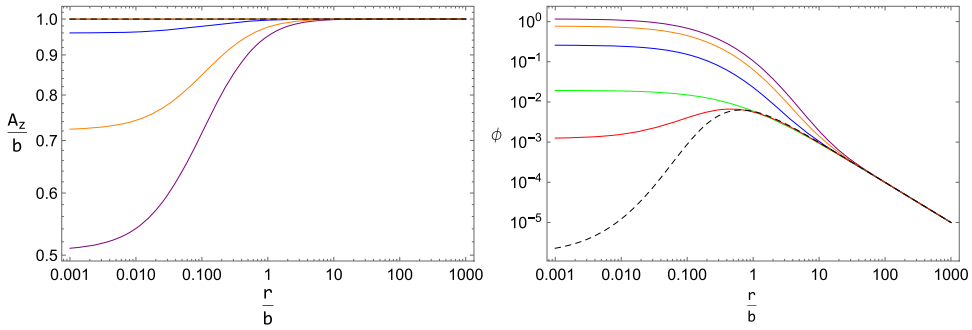

Fig. 2 Log-log plot of the bulk profile of A_z (left) and ϕ (right) for different graviton mass $m_g|c_2|/b$ at $M/b = 0.01$. As $m_g|c_2|/b$ is increased from 0 to 7, the gauge field A_z changes from top to bottom while the scalar field ϕ changes from bottom to top

which will be confirmed from the critical point of the phase transition studied in the next section.

3 Effects of massive gravity on phase transition

In this section, we will explore the effects of graviton mass on the transport properties of the holographic Weyl semimetals. We will compute the anomalous Hall conductivity and obtain the phase diagram of the system. We will discuss the spontaneous symmetry breaking solution at $M/b = 0$ for large graviton mass. We will also study the longitudinal and transverse conductivity.

Using the Kubo formula, the conductivities of the dual field theory reads

$$\sigma_{ij} = \lim_{\omega\to 0} \frac{1}{i\omega} \langle J_i J_j \rangle_R(\omega, \mathbf{k} = 0)\,, \tag{3.1}$$

where the current-current retarded Green's functions can be computed by studying the bulk gauge field fluctuations with ingoing boundary condition at the horizon.

The vector gauge field perturbations take the form

$$\delta V_x = v_x(r)e^{-i\omega t}, \delta V_y = v_y(r)e^{-i\omega t}, \delta V_z = v_z(r)e^{-i\omega t}\,, \tag{3.2}$$

Note that, the vector gauge field fluctuations decouple from the metric fluctuations. Therefore, the situation here is different with the finite density cases in [39,44,45]. For finite density system, the non-zero graviton mass terms usually affect the physics of the system in two ways [39]. First, in thermal equilibrium, the background geometry is altered by the non-zero mass terms and especially the near horizon geometry becomes $AdS_2 \times \mathbb{R}^d$ in the zero-temperature limit. Second, at the level of linearised perturbations, the dynamical degree of freedoms are increased and the dual energy momentum tensor is not conserved due to the non-zero graviton mass terms. In contrast, as the holographic Weyl semimetals is a zero density system, the decoupling of vector gauge field fluctuations with the metric fluctuations indicates that the effects of non-zero mass terms on the transports arise through their effects on the equilibrium solutions.[7]

Plugging (3.2) into the vector gauge field equation, we obtain

$$v_z'' + \left(\frac{u'}{u} + \frac{f'}{f} - \frac{h'}{2h}\right)v_z' + \frac{\omega^2}{u^2}v_z = 0\,, \tag{3.3}$$

$$v_\pm'' + \left(\frac{u'}{u} + \frac{h'}{2h}\right)v_\pm' + \frac{\omega^2}{u^2}v_\pm \pm 8\alpha\omega\frac{A_z'}{u\sqrt{h}}v_\pm = 0\,, \tag{3.4}$$

where $v_\pm = v_x \pm i v_y$. Since we are interested in the DC conductivities, we will use the near-far matching method [12] to compute these quantities. Finally, the DC conductivities σ_{xx}, σ_{yy} and σ_{xy} reads

$$\begin{aligned}\sigma_T &= \sigma_{xx} = \sigma_{yy}\\ &= \frac{G_+ + G_-}{2i\omega} = \sqrt{h(r_h)},\\ \sigma_{xy} &= \frac{G_+ - G_-}{2\omega}\\ &= 8\alpha\big(b - A_z(r_h)\big)\,,\end{aligned} \tag{3.5}$$

where $G_\pm = \omega\big(\pm 8\alpha(b - A_z(r_h)) + i\sqrt{h(r_h)}\big)$ is the Green functions of $v_\pm$. Similarly, the longitudinal conductivity σ_{zz} is given by

$$\sigma_{zz} = \frac{G_{zz}}{i\omega} = \frac{f(r_h)}{\sqrt{h(r_h)}}\,, \tag{3.6}$$

The anomalous Hall conductivity for the consistent current reads

$$\sigma_{\text{AHE}} = 8\alpha b - \sigma_{xy} = 8\alpha A_z(r_h)\,, \tag{3.7}$$

3.1 Anomalous Hall conductivity

We will now study the anomalous Hall conductivity. Figure 3 shows the anomalous Hall conductivity as a function of M/b at $T/b = 0.03$, where each curve corresponds to different graviton mass $m_g|c_2|/b$. For the translation invariant

[7] Instead, the axial gauge field fluctuations will necessary involve the metric fluctuations. It will be interesting to investigate the axial conductivity in the presence of non-zero mass terms and verify the 1/3 relation between axial Hall conductivity and electric Hall conductivity found in [22].

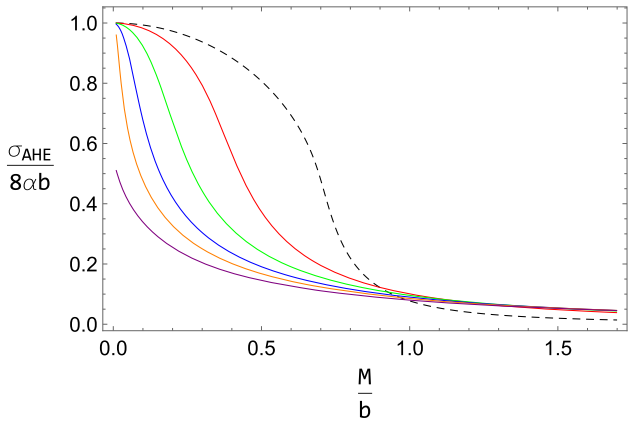

Fig. 3 The anomalous Hall conductivity as a function of M/b for different graviton mass $m_g|c_2|/b$ at $T/b = 0.03$. The black dashed line is for the massless case, while the colored solid line are for graviton mass $m_g|c_2|/b = 0.5$ (red), 1.5 (green), 3 (blue), 4.5 (orange), 7 (purple) from right to left respectively

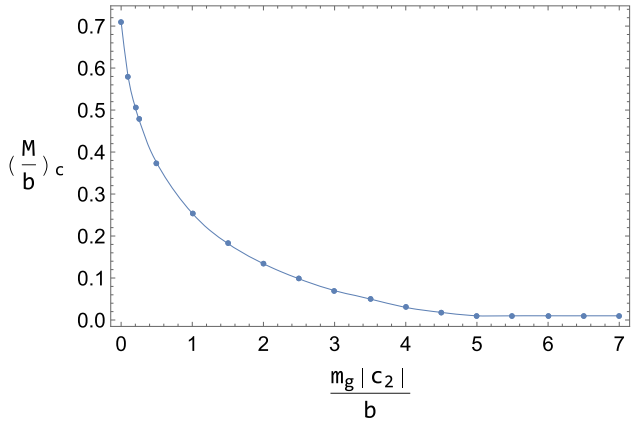

Fig. 4 The critical point as a function of graviton mass $m_g|c_2|/b$ at $T/b = 0.03$

Table 1 The instability condition for scalar field perturbations

	$T/b = 0$	$T/b = 0.03$
$m_g\|c_2\|/b$	1	5.45

case (zero graviton mass), as M/b is increased, the (normalized) anomalous Hall conductivity decreases monotonically from 1 in the Weyl semimetal phase to a very small value in the topological trivial phase. For a non-zero graviton mass, we find a similar monotonically decreasing behavior with the increasing of M/b. The anomalous Hall conductivity decreases rapidly and becomes negligible at large value of M/b. As the graviton mass becomes large, the anomalous Hall conductivity still decrease monotonically. However, near $M/b \approx 0$, its value is less than 1 and decreases with the increasing of graviton mass.[8]

To characterise the effects of non-zero graviton mass terms on the properties of phase transition, we will also study the critical point $(M/b)_c$ as a function of graviton mass. The critical value of the phase transition is encoded in the anomalous Hall conductivity, which is the point with maximum $|\frac{\partial\sigma_{AHE}}{\partial(M/b)}|$. Figure 4 shows that as the graviton mass is increased, the critical value $(M/b)_c$ decreases monotonically. Above a critical graviton mass with $m_g|c_2|/b \approx 5$, the critical value $(M/b)_c$ goes to zero. Note that, the Weyl semimetal phase is characterized by the non-zero anomalous Hall conductivity and exists for $M/b < (M/b)_c$. Therefore, the behavior of critical point shows that the non-zero graviton mass terms can destroy the Weyl points and reduce the region of Weyl semimetal phase.

The phenomena described above are similar to that of axion fields induced momentum relaxation studied in Ref. [32]. Note that, the massive gravity and axion model are different approaches for translation symmetry breaking and momentum relaxation. Therefore, regardless of the different mechanism of translational symmetry breaking in these two models, their effects of momentum relaxation on the holographic Weyl semimetals are universal.

All these phenomena are also consistent with the predictions from weakly coupled field theory [3]. We will now give an intuitive picture, similar to the Ref. [32], to explain it.[9] The explanation starts by relating k_L (the width of Brillouin zone) to the graviton mass $m_g|c_2|/b$, and we fix the distance between Weyl points to be 1. Thus, it is natural to expect that k_L will decrease with the increasing of graviton mass, as the massless case corresponds to translation invariance with $k_L \to \infty$. Therefore, there exists a critical $m_g|c_2|/b$ to make $k_L = 1$ where the two Weyl points meet at the boundary of Brillouin zone and annihilate with each other. The disappearance of the Weyl semimetal phase can be understood as a result of the annihilation of Weyl points.

3.2 Spontaneous symmetry breaking solutions at $M/b = 0$

To explain the behavior of anomalous Hall conductivity near $M/b \approx 0$, we will discuss two solutions of the background system at $M/b = 0$. First, we have an analytical solution [46]

$$u = r^2 - \frac{r_h^4}{r^2} + \frac{Fm_g^2c_1}{3}r\left(1 - \frac{r_h^3}{r^3}\right)$$

[8] We will explain this point in the following subsection.

[9] There are opinions that the massive gravity captures the phenomenon of disorder in field theory. One may interpret the phenomenon here as disorder-induced localization for the topological degrees of freedom. We thank Francisco Pena-Benitez for pointing out this.

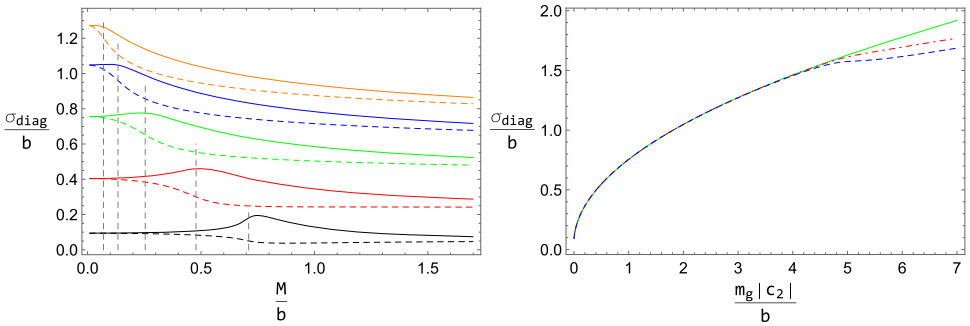

Fig. 5 Left: the transverse (solid lines) and longitudinal (dashed lines) conductivities as a function of M/b for different graviton mass at $T/b = 0.03$. The plot is for $m_g|c_2|/b = 0$ (black), 0.25 (red), 1 (green), 2 (blue), 3 (orange). The dashed gray lines are the location of critical points of the phase transition. Right: the diagonal conductivities as a function of graviton mass. The green line is for the analytical result at $M/b = 0$, while the red (blue) dashed lines are for numerical results of transverse (longitudinal) conductivities at $M/b = 0.01$

$$+F^2 m_g^2 c_2 \left(1-\frac{r_h^2}{r^2}\right)+\frac{2F^3 m_g^2 c_3}{r}\left(1-\frac{r_h}{r}\right),$$
$$f = h = r^2, \qquad A_z = b,$$
$$\phi = 0, \tag{3.8}$$

Note that, this solution is equal to the analytical solution in Ref. [32], if we choose $c_2 = -\frac{\beta^2}{4F^2 m_g^2}$ and $c_1 = c_3 = 0$. It is worth noting that, only in the isotropic case (i.e. $f = h$), the background solutions are the same for the $\mathcal{U}_2$ sector of massive gravity and the axion model.[10] From (3.7), we obtain $\frac{\sigma_{AHE}}{8\alpha b}|_{M=0} = 1$, which is different from the numerical results in Fig. 3 at large graviton mass near $M/b \approx 0$.

Second, in addition to the analytical solution (3.8), the system also has a spontaneous symmetry breaking (SSB) solution. This comes from the observation that the zero temperature near-horizon limit of (3.8) is $AdS_2 \times \mathbb{R}^3$. At zero temperature, the near horizon expansion of metric function takes $u = u_2(r-r_h)^2 + \cdots = (2 - c_2 F^2 m_g^2/r_h^2 - 2c_3 F^3 m_g^2/r_h^3)(r-r_h)^2 + \cdots$. By analyzing the scalar field fluctuations following [48], its effective mass near the AdS_2 horizon reads $m_{eff}^2 = \frac{m^2}{u_2} + \frac{b^2 q^2}{r_h^2 u_2}$. Thus, if the effective mass is below the Breitenlohner-Freedman (BF) bound of AdS_2, i.e. $m_{eff}^2 < m_{BF}^2 = -1/4$, the scalar field perturbations are unstable. This instability indicates the existence of new phases with non-trivial ϕ, which can be identified as a spontaneous symmetry breaking solution. The condition for instability can be computed analytically at zero temperature, which is determined by $m_g|c_i|/b$. As we turn on the temperature and keep T/b fixed, there exists a critical $m_g|c_i|/b$ above which the SSB solution appears at $M/b = 0$. We show the condition for instability in the table for $m_g|c_2|/b$.

In summary, there exist two branches of background solutions at $M/b = 0$ for large graviton mass. When $m_g|c_2|/b$ is bigger than the critical value shown in the table, the background solutions approach to the spontaneous symmetry breaking solution in the $M/b \to 0$ limit. Therefore, its anomalous Hall conductivity will deviate 1 and generally depend on $m_g|c_2|/b$, as is shown in Fig. 3 for $M/b \to 0$. However, a detailed analysis of the physics near $M/b = 0$ is beyond the scope of this paper and demands more works.

3.3 Transverse and longitudinal conductivities

Apart from the anomalous Hall conductivity, it is interesting to study the transverse (σ_T) and longitudinal (σ_L) conductivities as a function of M/b for different graviton mass, which is shown in the left plot Fig. 5. For fixed graviton mass, the σ_T and σ_L have a same value at $M/b = 0.01$. Then with the increasing of M/b, the σ_T increase while the σ_L decrease. At the intermediate range of M/b, the σ_T produces a peak while the σ_L produces a minimal. Finally, they both approach to a constant value at large M/b. On the other hand, as we increase the graviton mass, the diagonal conductivities are increased. Especially, the peak and minimal of the diagonal conductivities move to a small value of M/b with the increasing of graviton mass, which is similar to the behavior of critical point of the phase transition.

At $M/b = 0.01$, the σ_T and σ_L are equal, which can be compared to the conductivities obtained from the analytical solution (3.8) (i.e. $\sigma_{\text{diag}} = \frac{1}{2}\left(\pi T + \sqrt{\pi^2 T^2 - 2c_2}\right)$). In the right plot of Fig. 5, we show the diagonal conductivities as a function of graviton mass for numerical results at $M/b = 0.01$ and the analytical results at $M/b = 0$. As the graviton mass is increased, the numerical results are equal to the analytical results. However, for large graviton mass, the numerical conductivities departure from the analytical conductivities, which is due to the appearance of spontaneous symmetry breaking solution discussed in the previous subsection. In summary, the behavior of diagonal conduc-

[10] Similarly, the solution of massive gravity can also be mapped to that of conformal gravity in 4d [47].

tivities under momentum relaxation is consistent with the phenomenon we found in anomalous Hall conductivity.

4 Conclusion and discussion

In this work, we have studied the effects of momentum relaxation on the holographic Weyl semimetals, which is characterized by a quantum phase transition between the Weyl semimetal phase and a topological trivial phase. The momentum relaxation in field theory is induced by the non-zero graviton mass terms. By tuning the graviton mass, we have computed the anomalous Hall conductivity as a function of M/b, which further determines the critical value of the phase transition. We have found that the critical value decreases with the increasing of graviton mass and finally goes to zero above a critical graviton mass. This phenomenon is qualitatively similar to the results in Ref. [32], indicating a universal phenomenon in the momentum relaxed holographic Weyl semimetals, which is also consistent with the predictions from the weakly coupled field theory. We have also pointed out the existence of a spontaneous symmetry breaking solution at $M/b = 0$, which interprets the deviation of anomalous Hall conductivity from 1 near $M/b = 0$ at large graviton mass.

Notably, the physics described above has also evidenced from the behavior of diagonal conductivity, where the peak (minimal) in the transverse (longitudinal) conductivity goes to zero as the graviton mass is increased. We have also studied the diagonal conductivities as function of graviton mass at small M/b and compared it with the analytical result at $M/b = 0$.

Our study of momentum relaxation in holographic Weyl semimetals reveals interesting and universal phenomenon of the system, and there are several directions that are worth the further study. First, it is natural to study the zero temperature ground-state of the holographic Weyl semimetals in the presence of non-zero graviton mass terms, which is important to reveal the underlying physics. Second, as the vector gauge field fluctuations studied in this paper decouple from the metric fluctuations, the d.c. conductivities are encoded in the equilibrium solutions. Thus, it will be interesting to study the axial gauge field fluctuations to see the effects of graviton mass at linear perturbation level.

Acknowledgements We thank Yan Liu for useful discussion and guidance throughout the project. We thank Yan Liu and Hong-Da Lyu for reading the draft and providing helpful comments. We thank Hong-Da Lyu, Francisco Pena-Benitez and Hai-Qing Zhang for discussion. This work is supported by the National Natural Science Foundation of China Grant no. 11875083.

Data Availability Statement This manuscript has no associated data or the data will not be deposited. [Authors' comment: This is a theoretical study and no experimental data was used.]

Funded by SCOAP[3].

Appendix A: Equations of motion and asymptotic expansions

Upon setting $2\kappa^2 = L = 1$, the background equations of motion for the ansatz (2.2) are

$$
\begin{aligned}
&\frac{u''}{u} - \frac{f''}{f} + \frac{h'}{2h}\left(\frac{u'}{u} - \frac{f'}{f}\right) \\
&+ \frac{m_g^2\left(6F^2F_z c_3\sqrt{h} + 2FF_z c_2\sqrt{fh} + 2F^2c_2 h + Fc_1\sqrt{fh}\right)}{ufh} = 0\,, \\
&\frac{u''}{2u} + \frac{f''}{f} + \frac{u'f'}{uf} - \frac{f'^2}{4f^2} - \frac{6}{u} - \frac{A_z'^2}{4h} \\
&+ \frac{\phi^2}{2u}\left(m^2 + \frac{\lambda}{2}\phi^2 - \frac{q^2A_z^2}{h}\right) \\
&+ \frac{\phi'^2}{2} - \frac{m_g^2\left(F^2c_2 + Fc_1\sqrt{f}\right)}{uf} = 0\,, \\
&\frac{6}{u} - \frac{u'}{2u}\left(\frac{f'}{f} + \frac{h'}{2h}\right) - \frac{f'h'}{2fh} \\
&- \frac{f'^2}{4f^2} + \frac{A_z'^2}{4h} - \frac{\phi^2}{2u}\left(m^2 + \frac{\lambda}{2}\phi^2 + \frac{q^2A_z^2}{h}\right) + \frac{\phi'^2}{2} \\
&+ \frac{m_g^2\left(6F^2F_z c_3\sqrt{h} + 4FF_z c_2\sqrt{fh} + 2F^2c_2 h + 2Fc_1\sqrt{fh} + F_z c_1 f\sqrt{h}\right)}{2ufh} = 0\,, \\
&A_z'' + \left(\frac{u'}{u} + \frac{f'}{f} - \frac{h'}{2h}\right)A_z' - \frac{2q^2\phi^2}{u}A_z = 0\,, \\
&\phi'' + \left(\frac{u'}{u} + \frac{f'}{f} + \frac{h'}{2h}\right)\phi' \\
&- \left(\frac{q^2A_z^2}{uh} + \frac{m^2}{u}\right)\phi - \frac{\lambda\phi^3}{u} = 0\,,
\end{aligned}
$$

where the prime denotes the derivative of radial coordinate r. Note that, in contrast to the minimal model [12], the above equations of motion contain new terms proportional to the graviton mass. Meanwhile, in the presence of non-zero graviton mass terms, the scaling symmetries involve the scaling of the reference metric. Particularly, there are three scaling symmetries

$$
\begin{aligned}
&\text{(I.)}\ \ (x, y) \to \gamma(x, y),\ \ f \to \gamma^{-2} f,\ \ F \to \gamma^{-1} F\,; \\
&\text{(II.)}\ \ z \to \gamma z,\ \ h \to \gamma^{-2} h,\ \ (A_z, F_z) \to \gamma^{-1}(A_z, F_z)\,; \\
&\text{(III.)}\ \ r \to \gamma r,\ \ (t, x, y, z) \to \gamma^{-1}(t, x, y, z),\ \ (u, f, h) \to \\
&\qquad \gamma^2(u, f, h),\ \ (A_z, F, F_z) \to \gamma(A_z, F, F_z);
\end{aligned}
$$

A.1 Near horizon expansions

At the black hole horizon, we take the ansatz

$$
\begin{aligned}
u &= 4\pi T(r-r_h)+\cdots,\\
f &= f_0+\Big[\frac{4F^3}{\sqrt{h_0}}m_g^2c_3+\Big(2F^2+\frac{2F^2\sqrt{f_0}}{\sqrt{h_0}}\Big)m_g^2c_2\\
&\quad+\Big(\frac{Ff_0}{3\sqrt{h_0}}+\frac{5F\sqrt{f_0}}{3}\Big)m_g^2c_1\\
&\quad+f_0\Big(8-\frac{2m^2\phi_0^2}{3}-\frac{\lambda\phi_0^4}{3}\Big)\Big]\frac{(r-r_h)}{4\pi T}+\cdots,\\
h &= h_0+\Big[\frac{4F^3\sqrt{h_0}}{f_0}m_g^2c_3+\frac{4F^2\sqrt{h_0}}{\sqrt{f_0}}m_g^2c_2\\
&\quad+\Big(\frac{4F\sqrt{h_0}}{3}+\frac{2Fh_0}{3\sqrt{f_0}}\Big)m_g^2c_1\\
&\quad+h_0\Big(8-\frac{2m^2\phi_0^2}{3}-\frac{\lambda\phi_0^4}{3}\Big)\\
&\quad-2q^2A_{z0}^2\phi_0^2\Big]\frac{(r-r_h)}{4\pi T}+\cdots,\\
A_z &= A_{z0}+\frac{q^2A_{z0}\phi_0^2}{2\pi T}(r-r_h)+\cdots,\\
\phi &= \phi_0+\frac{\phi_0\big(q^2A_{z0}^2+h_0(m^2+\lambda\phi_0^2)\big)}{4h_0\pi T}(r-r_h)+\cdots,
\end{aligned}
$$

Note that, we have set $F_z = F$ in the above expansions. The independent parameters in the expansions are $T, r_h, f_0, h_0, A_{z0}, \phi_0, c_i (i = 1, 2, 3)$, which can be reduced by the above scaling symmetries and are mapped into dimensionless parameters $(\frac{M}{b}, \frac{T}{b}, \frac{m_g c_i}{b})$ in the field theory. Therefore, the numerical solutions can be obtained by integrating the background equations from the horizon to the AdS boundary by properly choosing the shooting parameters.

A.2 Asymptotic boundary expansions

Close to the conformal boundary, i.e. $r \to \infty$, we have

$$
\begin{aligned}
u &= r^2+\frac{c_1Fm_g^2r}{3}-\frac{M^2}{3}\\
&\quad+c_2F^2m_g^2+\frac{c_1Fm_g^2M^2+12c_3F^3m_g^2}{6r}\\
&\quad+\frac{(3\lambda+2)M^4\ln r}{18r^2}+\frac{u_2}{r^2}\cdots,\\
f &= r^2-\frac{M^2}{3}+\frac{8c_1Fm_g^2M^2}{27r}\\
&\quad+\Big[\frac{(3\lambda+2)M^4}{18}-\frac{2c_1^2F^2m_g^4M^2}{27}+\frac{c_2F^2m_g^2M^2}{6}\Big]\frac{\ln r}{r^2}\\
&\quad+\frac{f_2}{r^2}+\cdots,\\
h &= r^2-\frac{M^2}{3}+\frac{8c_1Fm_g^2M^2}{27r}\\
&\quad+\Big[\frac{(3\lambda+2)M^4}{18}+\frac{q^2b^2M^2}{2}\\
&\quad-\frac{2c_1^2F^2m_g^4M^2}{27}+\frac{c_2F^2m_g^2M^2}{6}\Big]\frac{\ln r}{r^2}\\
&\quad+\frac{h_2}{r^2}+\cdots,\\
A_z &= b-bq^2M^2\frac{\ln r}{r^2}+\frac{\eta}{r^2}+\cdots,\\
\phi &= \frac{M}{r}-\frac{2c_1Fm_g^2M}{3r^2}\\
&\quad-\Big[\frac{(3\lambda+2)M^3}{6}+\frac{Mb^2q^2}{2}\\
&\quad-\frac{2c_1^2F^2m_g^4M}{9}+\frac{c_2F^2m_g^2M}{2}\Big]\frac{\ln r}{r^3}\\
&\quad+\frac{O}{r^3}+\cdots,
\end{aligned}
$$

with $h_2 = -2f_2+\frac{1}{8}b^2M^2q^2+\frac{7M^4}{36}+\frac{\lambda M^4}{8}-MO-\frac{19}{54}c_1^2F^2m_g^4M^2+\frac{1}{8}c_2F^2m_g^2M^2$. Note that, we have set $F_z = F$ to get this expansions. It is worth noting that the metric functions acquire nontrivial terms in the presence of nonzero graviton mass terms. In contrast to the minimal model of holographic Weyl semimetals [12], the two conserved charges no longer exist under momentum relaxation. Therefore, we can not express u_2, f_2 and h_2 in the metric expansions in terms of M, O, b and η. Furthermore, the above expansions are determined up to a radial shift $r \to r + a$.

Appendix B: Thermodynamics

The Euclidean action reads

$$
S_{\mathrm{E}} = -\int d^5x\sqrt{-g}\mathcal{L}, \tag{B.1}
$$

From the symmetry of the background ansatz (2.2), we can observe that the tt component of χ_{ab} and T_{ab} only contain terms proportional to the metric. Therefore, the tt component of Einstein equation can be simplified as

$$
R_{tt} = \frac{1}{2}g_{tt}\mathcal{L}, \tag{B.2}
$$

Therefore, the on shell action is a total derivative

$$
\begin{aligned}
S_{\mathrm{E}} &= -\int d^4x\int_{r_h}^{r_\infty}dr\sqrt{-g}(2R^t{}_t)\\
&= \int d^4x\int_{r_h}^{r_\infty}dr[u'f\sqrt{h}]'\\
&= \int d^4x\Big[u'f\sqrt{h}\Big|_{r_\infty}-u'f\sqrt{h}\Big|_{r_h}\Big],
\end{aligned} \tag{B.3}
$$

Note that, the above expression is divergent near the AdS boundary. To compute the free energy, one need to add boundary counterterms, which takes the form

$$S_{\rm ROS} = S_{\rm E} + S_{\rm GH} + S_{\rm c.t.}, \tag{B.4}$$

where the Gibbons–Hawking term

$$S_{\rm GH} = \frac{1}{\kappa^2}\int d^4x\sqrt{-\gamma}K\,,$$

and the counterterm

$$\begin{aligned} S_{\rm c.t.} = \frac{1}{2\kappa^2}\int d^4x\sqrt{-\gamma}\Big[& -6-\Phi^2+\log(r) \\ & \Big(\frac{1}{4}\mathcal{F}_{\mu\nu}\mathcal{F}^{\mu\nu}+\frac{1}{4}F_{\mu\nu}F^{\mu\nu} \\ & +|D_\mu\Phi|^2+\lambda_b\Phi^4\Big) \\ & -\frac{m_g^2c_1}{3}\hat{\mathcal{U}}_1 \\ & -\Big(\frac{m_g^2c_2}{2}-\frac{m_g^4c_1^2}{72}\Big)\hat{\mathcal{U}}_2 \\ & -\Big(m_g^2c_3-\frac{m_g^4c_1c_2}{12}+\frac{m_g^6c_1^3}{432} \\ & -\frac{M^2m_g^2c_1}{12F^2}\Big)\hat{\mathcal{U}}_3\Big]\,, \end{aligned}$$

Note that, $\lambda_b = \frac{1}{3}+\frac{\lambda}{2}-\frac{4m_g^4c_1^2F^2}{9M^2}+\frac{m_g^2c_2F^2}{M^2}$ and $\hat{\mathcal{U}}_i\,(i=1,2,3)$ are graviton mass terms written in terms of induced metric γ_{ij}. The coefficients of each terms can be determined by demanding that the renormalized on-shell action is finite. Note that the counterterms of massive gravity herein are sufficient to cancel the divergence coming from the bulk graviton mass terms and see Ref. [49] for more systematic treatment. Interestingly, in the presence of non-zero graviton mass terms, the counterterm of scalar field is slightly different.

Having substituted the asymptotic expansions, we can obtain the renormalized on-shell action $S_{\rm ROS}$. Consequently, the free energy reads

$$\begin{aligned} \frac{\Omega}{V} &= -\frac{S_{\rm ROS}}{V} \\ &= \frac{7M^4}{36}-2MO-Ts-3u_2 \\ &\quad -\frac{23}{72}m_g^4c_1^2F^2M^2-\frac{1}{2}m_g^2c_2F^2M^2 \\ &\quad +m_g^4c_1c_3F^4+\frac{3}{4}m_g^4c_2^2F^4 \\ &\quad -\frac{1}{8}m_g^6c_1^2c_2F^4+\frac{5m_g^8c_1^4F^4}{1728}. \end{aligned} \tag{B.5}$$

where $s = 4\pi f_0\sqrt{h_0}$ is the entropy density.

The expectation value of the boundary stress tensor reads

$$T_{\mu\nu} = 2(K_{\mu\nu}-K\gamma_{\mu\nu})+\frac{2}{\sqrt{-\gamma}}\frac{\delta S_{\rm c.t.}}{\delta\gamma^{\mu\nu}}\,, \tag{B.6}$$

Therefore, the energy density is

$$\begin{aligned} \epsilon = T^0_0 = & \frac{7M^4}{36}-2MO-3u_2 \\ & -\frac{23}{72}m_g^4c_1^2F^2M^2-\frac{1}{2}m_g^2c_2F^2M^2 \\ & +m_g^4c_1c_3F^4+\frac{3}{4}m_g^4c_2^2F^4 \\ & -\frac{1}{8}m_g^6c_1^2c_2F^4+\frac{5m_g^8c_1^4F^4}{1728}. \end{aligned} \tag{B.7}$$

Consequently, the thermodynamics relation $\frac{\Omega}{V} = \epsilon - Ts$ holds.

References

1. N.P. Armitage, E.J. Mele, A. Vishwanath, Weyl and Dirac semimetals in three dimensional solids. Rev. Mod. Phys. **90**, 015001 (2018). https://doi.org/10.1103/RevModPhys.90.015001. arXiv:1705.01111
2. A.A. Burkov, M.D. Hook, L. Balents, Topological nodal semimetals. Phys. Rev. B **84**, 235126 (2011). https://doi.org/10.1103/PhysRevB.84.235126. arXiv:1110.1089
3. P. Hosur, X. Qi, Recent developments in transport phenomena in Weyl semimetals. Comptes Rendus Physique **14**, 857 (2013). https://doi.org/10.1016/j.crhy.2013.10.010. arXiv:1309.4464
4. K. Landsteiner, Notes on anomaly induced transport. Acta Phys. Pol. B **47**, 2617 (2016). https://doi.org/10.5506/APhysPolB.47.2617. arXiv:1610.04413
5. R.M.A. Dantas, F. Pena-Benitez, B. Roy, P. Surowka, Non-Abelian anomalies in multi-Weyl semimetals. Phys. Rev. Res. **2**, 013007 (2020). https://doi.org/10.1103/PhysRevResearch.2.013007. arXiv:1905.02189
6. M.N. Chernodub, Y. Ferreiros, A.G. Grushin, K. Landsteiner, M.A.H. Vozmediano, Thermal transport, geometry, and anomalies. arXiv:2110.05471
7. J. Zaanen, Electrons go with the flow in exotic material systems. Science **351**, 1026 (2016). https://doi.org/10.1126/science.aaf2487
8. J. Gonzalez, Strong-coupling phases of 3D Dirac and Weyl semimetals. A renormalization group approach. JHEP **10**, 190 (2015). https://doi.org/10.1007/JHEP10(2015)190. arXiv:1509.00210
9. J. Zaanen, Y.W. Sun, Y. Liu, K. Schalm, *Holographic Duality in Condensed Matter Physics*, (Cambridge University Press, 2015). http://www.cambridge.org/de/academic/subjects/physics/condensed-matter-physics-nanoscience-and-mesoscopic-physics/holographic-duality-condensed-matter-physics?format=HB#AlwhgydkVTSFfv7H.97
10. M. Ammon, J. Erdmenger, *Gauge/gravity Duality: Foundations and Applications*, (Cambridge University Press, 2015). http://www.cambridge.org/de/academic/subjects/physics/theoretical-physics-and-mathematical-physics/gaugegravity-duality-foundations-and-applications#xOzmEecLSr4ZJFIH.97
11. S.A. Hartnoll, A. Lucas, S. Sachdev, Holographic quantum matter. arXiv:1612.07324

12. K. Landsteiner, Y. Liu, Y.W. Sun, Quantum phase transition between a topological and a trivial semimetal from holography. Phys. Rev. Lett. **116**, 081602 (2016). https://doi.org/10.1103/PhysRevLett.116.081602. arXiv:1511.05505
13. K. Landsteiner, Y. Liu, The holographic Weyl semi-metal. Phys. Lett. B **753**, 453 (2016). https://doi.org/10.1016/j.physletb.2015.12.052. arXiv:1505.04772
14. U. Gursoy, V. Jacobs, E. Plauschinn, H. Stoof, S. Vandoren, Holographic models for undoped Weyl semimetals. JHEP **04**, 127 (2013). https://doi.org/10.1007/JHEP04(2013)127. arXiv:1209.2593
15. V. Jacobs, P. Betzios, U. Gursoy, H. Stoof, Electromagnetic response of interacting Weyl semimetals. Phys. Rev. B **93**, 195104 (2016). https://doi.org/10.1103/PhysRevB.93.195104. arXiv:1512.04883
16. K. Hashimoto, S. Kinoshita, K. Murata, T. Oka, Holographic Floquet states I: a strongly coupled Weyl semimetal. JHEP **05**, 127 (2017). https://doi.org/10.1007/JHEP05(2017)127. arXiv:1611.03702
17. K.B. Fadafan, A. O'Bannon, R. Rodgers, M. Russell, A Weyl semimetal from AdS/CFT with flavour. JHEP **04**, 162 (2021). https://doi.org/10.1007/JHEP04(2021)162. arXiv:2012.11434
18. M. Ammon, M. Heinrich, A. Jimenez-Alba, S. Moeckel, Surface states in holographic Weyl semimetals. Phys. Rev. Lett. **118**, 201601 (2017). https://doi.org/10.1103/PhysRevLett.118.201601. arXiv:1612.00836
19. Y. Liu, Y.W. Sun, Topological invariants for holographic semimetals. JHEP **10**, 189 (2018). https://doi.org/10.1007/JHEP10(2018)189. arXiv:1809.00513
20. K. Landsteiner, Y. Liu, Y.W. Sun, Odd viscosity in the quantum critical region of a holographic Weyl semimetal. Phys. Rev. Lett. **117**, 081604 (2016). https://doi.org/10.1103/PhysRevLett.117.081604. arXiv:1604.01346
21. G. Grignani, A. Marini, F. Pena-Benitez, S. Speziali, AC conductivity for a holographic Weyl Semimetal. JHEP **03**, 125 (2017). https://doi.org/10.1007/JHEP03(2017)125. arXiv:1612.00486
22. C. Copetti, J. Fernandez-Pendas, K. Landsteiner, Axial Hall effect and universality of holographic Weyl semi-metals. JHEP **02**, 138 (2017). https://doi.org/10.1007/JHEP02(2017)138. arXiv:1611.08125
23. Y. Liu, Y.W. Sun, Topological nodal line semimetals in holography. JHEP **12**, 072 (2018). https://doi.org/10.1007/JHEP12(2018)072. arXiv:1801.09357
24. M. Ammon, M. Baggioli, A. Jimenez-Alba, S. Moeckel, A smeared quantum phase transition in disordered holography. JHEP **04**, 068 (2018). https://doi.org/10.1007/JHEP04(2018)068. arXiv:1802.08650
25. M. Baggioli, B. Padhi, P.W. Phillips, C. Setty, Conjecture on the Butterfly Velocity across a Quantum Phase Transition. JHEP **07**, 049 (2018). https://doi.org/10.1007/JHEP07(2018)049. arXiv:1805.01470
26. Y. Liu, J. Zhao, Weyl semimetal/insulator transition from holography. JHEP **12**, 124 (2018). https://doi.org/10.1007/JHEP12(2018)124. arXiv:1809.08601
27. X. Ji, Y. Liu, X.M. Wu, Chiral vortical conductivity across a topological phase transition from holography. Phys. Rev. D **100**, 126013 (2019). https://doi.org/10.1103/PhysRevD.100.126013. arXiv:1904.08058
28. G. Song, J. Rong, S.J. Sin, Stability of topology in interacting Weyl semi-metal and topological dipole in holography. JHEP **10**, 109 (2019). https://doi.org/10.1007/JHEP10(2019)109. arXiv:1904.09349
29. V. Juričić, I. Salazar Landea, R. Soto-Garrido, Phase transitions in a holographic multi-Weyl semimetal. JHEP **07**, 052 (2020). https://doi.org/10.1007/JHEP07(2020)052. arXiv:2005.10387
30. M. Baggioli, D. Giataganas, Detecting Topological Quantum Phase Transitions via the c-Function. Phys. Rev. D **103**, 026009 (2021). https://doi.org/10.1103/PhysRevD.103.026009. arXiv:2007.07273
31. Y. Liu, X.M. Wu, An improved holographic nodal line semimetal. JHEP **05**, 141 (2021). https://doi.org/10.1007/JHEP05(2021)141. arXiv:2012.12602
32. J. Zhao, Momentum relaxation in a holographic Weyl semimetal. Phys. Rev. D **104**, 066003 (2021). https://doi.org/10.1103/PhysRevD.104.066003. arXiv:2109.07215
33. X. Ji, Y. Liu, Y.W. Sun Y.L. Zhang, A Weyl-Z_2 semimetal from holography. arXiv:2109.05993
34. R. Rodgers, E. Mauri, U. Gürsoy, H.T.C. Stoof, Thermodynamics and transport of holographic nodal line semimetals. arXiv:2109.07187
35. K. Landsteiner, Y. Liu, Y.W. Sun, Holographic topological semimetals. Sci. China Phys. Mech. Astron. **63**, 250001 (2020). https://doi.org/10.1007/s11433-019-1477-7. arXiv:1911.07978
36. G.T. Horowitz, J.E. Santos, D. Tong, Optical conductivity with holographic lattices. JHEP **07**, 168 (2012). https://doi.org/10.1007/JHEP07(2012)168. arXiv:1204.0519
37. Y. Liu, K. Schalm, Y.W. Sun, J. Zaanen, Lattice potentials and fermions in holographic non fermi-liquids: hybridizing local quantum criticality. JHEP **10**, 036 (2012). https://doi.org/10.1007/JHEP10(2012)036. arXiv:1205.5227
38. A. Donos, S.A. Hartnoll, Interaction-driven localization in holography. Nat. Phys. **9**, 649–655 (2013). https://doi.org/10.1038/nphys2701. arXiv:1212.2998
39. D. Vegh, Holography without translational symmetry. arXiv:1301.0537
40. T. Andrade, B. Withers, A simple holographic model of momentum relaxation. JHEP **05**, 101 (2014). https://doi.org/10.1007/JHEP05(2014)101. arXiv:1311.5157
41. A. Donos, J.P. Gauntlett, Holographic Q-lattices. JHEP **04**, 040 (2014). https://doi.org/10.1007/JHEP04(2014)040. arXiv:1311.3292
42. M. Baggioli, K.Y. Kim, L. Li, W.J. Li, Holographic Axion Model: a simple gravitational tool for quantum matter. Sci. China Phys. Mech. Astron. **64**, 270001 (2021). https://doi.org/10.1007/s11433-021-1681-8. arXiv:2101.01892
43. C. de Rham, G. Gabadadze, A.J. Tolley, Resummation of Massive Gravity. Phys Rev Lett **106**, 231101 (2011). https://doi.org/10.1103/PhysRevLett.106.231101. arXiv:1011.1232
44. R.A. Davison, Momentum relaxation in holographic massive gravity. Phys. Rev. D **88**, 086003 (2013). https://doi.org/10.1103/PhysRevD.88.086003. arXiv:1306.5792
45. M. Blake, D. Tong, Universal Resistivity from Holographic Massive Gravity. Phys. Rev. D **88**, 106004 (2013). https://doi.org/10.1103/PhysRevD.88.106004. arXiv:1308.4970
46. R.G. Cai, Y.P. Hu, Q.Y. Pan, Y.L. Zhang, Thermodynamics of black holes in massive gravity. Phys. Rev. D **91**, 024032 (2015). https://doi.org/10.1103/PhysRevD.91.024032. arXiv:1409.2369
47. B.E. Panah, S.H. Hendi, Black hole solutions correspondence between conformal and massive theories of gravity. EPL **125**, 60006 (2019). https://doi.org/10.1209/0295-5075/125/60006. arXiv:1904.07670
48. G.T. Horowitz, M.M. Roberts, Zero temperature limit of holographic superconductors. JHEP **11**, 015 (2009). https://doi.org/10.1088/1126-6708/2009/11/015. arXiv:0908.3677
49. F. Chen, S.F. Wu, Y. Peng, Hamilton–Jacobi approach to holographic renormalization of massive gravity. JHEP **07**, 072 (2019). https://doi.org/10.1007/JHEP07(2019)072. arXiv:1903.02672